Cuminum Cyminum Extract- A Green Corrosion Inhibitor of S300 Steel in 1 M HCl

R. Idouhli; A. Abouelfida A. Benyaich A. Aityoub
Laboratory of Physical Chemistry of Materials and Environment, Department of Chemistry, University Cadi Ayyad, Faculty of Science Semlalia, BP 2390 Marrakech, Morocco

Abstract

The corrosion inhibition of steel S300 in 1M HCl by Extracts of Cuminum cyminum was investigated by using weight loss measurements, Potentiodynamic Polarization Curves and Electrochemical Impedance Spectroscopy (EIS). The polarization Curves reveal that extracts of *C. cyminum* is a mixed-type inhibitor. The results show that the inhibition efficiency increases with the increasing of extract concentration to reach 97.49 % at 1. 3 g/l and decreases with temperature. Cumin extract is adsorbed on the steel surface according Langmuir isotherm. The adsorption parameters, enthalpy and activation energy were determined. The effect of temperature was studied and discussed.

Keywords: Cumin, steel, Corrosion, inhibition.

1. Introduction

Corrosion is a natural process commonly defined as the deterioration of a metal or its properties because of a reaction with its environment. Corrosion can cause dangerous and expensive damage to petrochemical industries, bridges and public buildings etc. The cost of this phenomenon is very costly with 4 % of the Gross Domestic Product (GDP) of industrial countries [1-2]. Corrosion can cause loss of steel equipments intervening in industrial applications; much of this loss is due to the contact with acid solutions. The corrosion inhibitor is one of means to delay this phenomenon effects on the metallic surface. However, it is increasingly reluctant to use the substances that may harm the environment. Most of the ecological inhibitors are biodegradable, non-toxic, readily available, and considerably in plenty grown over the past two decades [3-4]. Those advantages have incited many scientists to examine natural substances as corrosion inhibitors such as Aquilaria Crassna Leaves Extracts [5], Chenopodium Ambrosioides Extracts [6], Zingiber Officinal Roscoe Extract [7], Psidium Guajava Leaf Extract [8], oils [6-9-10] and pure plant compounds [11-12]. The use of inhibitors with aims to protect steel from corrosion in acid solutions is required. It has been reported in many previous studies that that inhibitors containing organic compounds bearing heteroatom with high electron density like nitrogen, sulfur and oxygen atoms and these contribute greatly to the inhibition of corrosion via various mechanisms [13].

Seeds of the cumin plant *Cuminum cyminum* (*CC*) have been used in traditional medicine, flavor foods and added to fragrances [14]. The inhibitory action of *CC* extract as eco-friendly and naturally occurring substance on corrosion behavior of S300 steel has been studied by gravimetric and electrochemical techniques such as potentiodynamic polarization and electrochemical impedance.

This work is devoted to the study of the behavior of steel in 1 M hydrochloric acid medium and the effect of the CC extract as inhibitor.

2. Materials and methods

2.1 Preparation of extracts and solutions

The cumin seeds CC was collected from plants cultivated in the region of Rhamna, Morocco. The corresponding extract was produced by the maceration method in ethanol. In fact the dried cumin powdered (5g) as added to 100 ml of ethanol using magnetic agitation for 24 hours at room temperature. After filtration, the aqueous extract was used to inhibit the corrosion phenomenon. The solution of 1M of HCl was prepared by dilution of an analytical grade (37 %) hydrochloric acid using twice distilled water.

2.2 Weight loss measurement

Steel specimens with cylindrical shapes having a total area of 1.57 cm^2, were used in weight loss experiments. The chemical composition of working electrode (wt) was Fe (98.55%), C (0.15%), Mn (1.25%) and Si (0.05%). The area of the working electrode was pre-treated before the experiment by pleating with sandpaper (CSi, grade 600 and 1200) and thoroughly washed with bidistilled water an degreased with acetone. After weighting, the specimens were immersed in 100 ml tested solutions of 1 M hydrochloric acid. The immersion time for the weight loss varied between 1 h and 14 h at 293 K. The corrosion rate (V) was calculated by the following relation:

$$V = \frac{\Delta m}{St} \tag{1}$$

Where Δm (mg) is the mass loss, S (cm^2) the total area of specimen (1.57 cm^2) and t (h) is the immersion time. The percentage inhibition efficiency was calculated by:

$$E(\%) = \frac{V_1 - V_2}{V_1} * 100 \qquad (2)$$

Where V_1 and V_2 are the values of corrosion rate without and with inhibitor, respectively.

2.3 Electrochemical analysis

The electrochemical study was accomplished using a potentiostat PGZ100 piloted by voltamaster 4 software. This potentiostat is connected to a double-walled one-compartment cell with tree electrode configurations. A platinum electrode with 2 cm^2 surface area and AgCl/Ag were used as auxiliary and reference electrodes, respectively. The working electrode was the surface area exposed to the electrolyte 0.76 cm^2. The polarization curves were obtained in the range of -0.8 V to -0.2 V at a scanning rate of 0.001 $V.s^{-1}$. The Electrochemical Impedance Spectroscopy was conducted in frequencies ranging from 100 KHz to 10 mHz at open circuit potential by applying the signals of sine wave voltage of 0.01 V peak to peak. Before all experiments, the potential was stabilized during 30 min. The effect of temperature on the inhibitor performance was carried out in a temperature range of 293 at 323 K. Experiments are repeated three times to ensure the reproducibility.

2.4 Fourier Transform Infrared Spectroscopy (FTIR)

The test coupons of our materials were exposed in 100 ml of 1 M HCl with 1.3 g/l of CC extract for 1 h at 293 K and washed with bidistilled water. After washing, specimens were dried and examined using FT-IR (Vertex 70 sample compartement RT-DLa TGS) for their functional groups adsorbed. The spectra were recorded in the frequency range between 4000 and 400 cm^{-1}.

3. Results and Discussion

3.1 Fourier Transform Infrared Spectroscopy (FTIR) analysis

The chemical constituents that contribute to corrosion inhibition have specific functional groups. The cumin crude extract and the layer formed on the steel surface which is treated with 1.3 g/l CC extract in 1 M HCl were analyzed by FT-IR, the spectra obtained is displayed in Fig. 1. A broad band in the range of 3420 cm^{-1} can be assigned to the presence of superficial adsorbed water, stretching mode of O-H and/or N-H bond, and that in the range 2852 - 2979 cm^{-1} is related to C-H stretching vibration [15]. The strong band at 1652 cm^{-1} that moves at 1774 cm^{-1} is assigned to C=C and C=O stretching vibration. Owing to the conjugation effect of flavonoids of the CC extract, the C=O peak shifts from about 1700 cm^{-1} to lower wavenumber, C=C and C=O stretching vibration bands are superposed and indicated at 1650 and 1720 cm^{-1} , respectively[16].

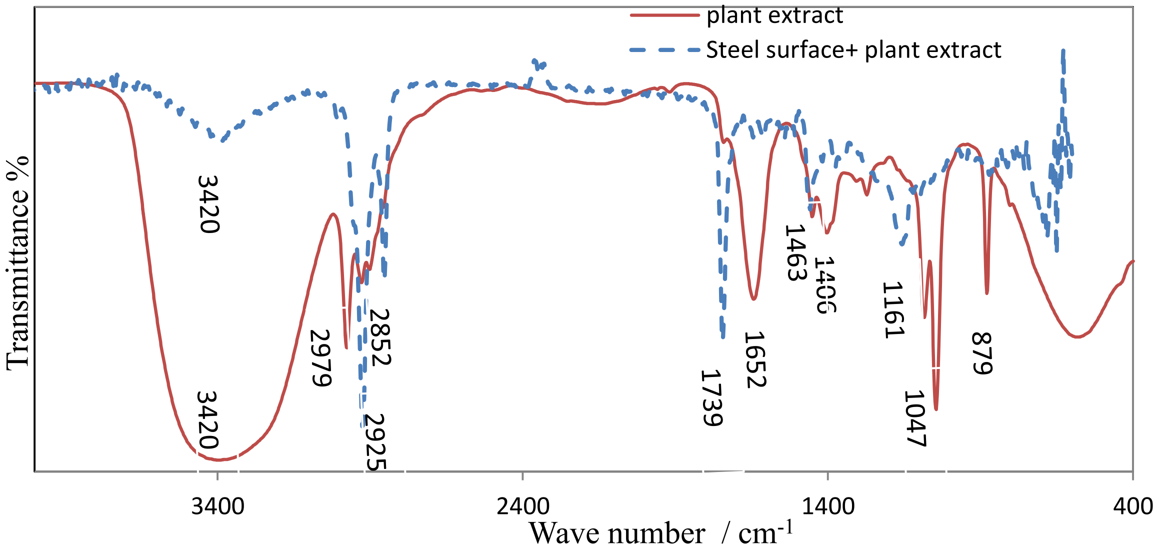

Fig. 1. Infrared spectra of CC extract and steel immersed in 1M HCl containing 1.3 g/l of CC extract.

The C-H bonds in $-CH_2$ and $-CH_3$ are indicated at 1406 and 1380 cm^{-1} respectively [17]. The bond at 1047-1161 cm^{-1} can be attributed to the C–N or C–O stretching vibration. Band at 682 cm^{-1} probably originates from $\gamma - Fe_2O_3$. The bands of CC extract are relatively more intense than the steel surface ones. These results indicate that the plant extract of CC contains O and N atoms in different functional groups and the same aromatic rings. This is showing that the inhibiting film consist of a small amount of extract complex with steel and the iron oxides.

3.2 Corrosion study

3.2.1 Weight loss measurements

Fig 2 presents the evolution of weight loss and the inhibition efficiency (E%) of steel immersed in 1M hydrochloric acid solution at 293 K versus the immersion time (h). Additions of CC extract increases the inhibition efficiency and hence decreases the weight loss of the steel. The inhibition is estimated about 80.90 % after 14 h of time immersion with 1.3 g/l of CC extract.

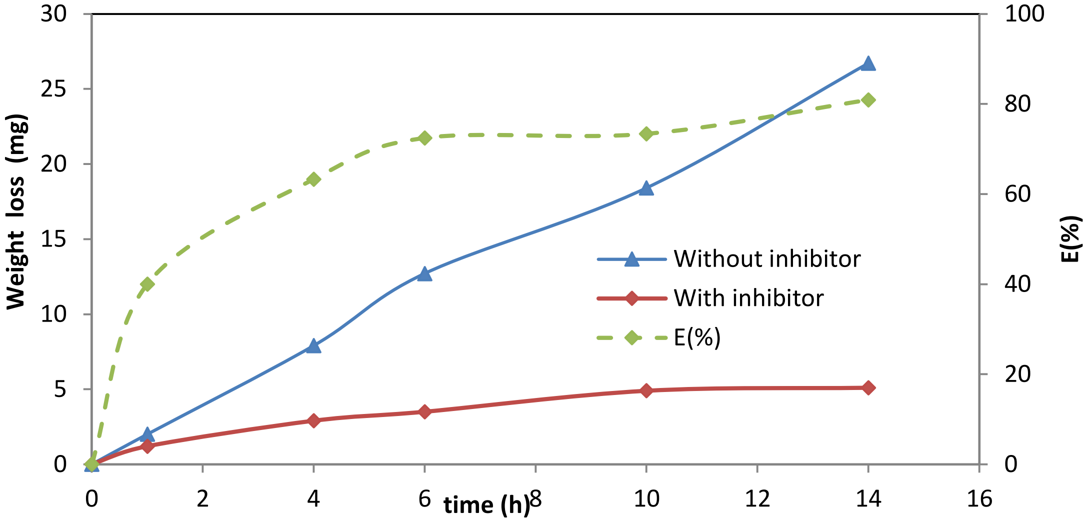

Fig. 2.Weight loss and inhibition efficiency plots of steel immersed in 1M hydrochloric acid solution with and without CC extract at 293k versus the immersion time (h)

The result obtained shows high weight loss in 1M hydrochloric acid solution. The addition of CC extract to the solution reduces the weight loss. The difference in weight loss between the medium with and without CC extract is more important after 6 h, which explains that the CC extract is effective as inhibitor for steel in 1M HCl at 293k. These results agree with those realized by Obiukwu and Osita [18, 19].

The results show that as the time immersion increases, the weight loss decreases and therefore the inhibition efficiency increases. These explain that this inhibitor acts through adsorption on steel surface and formation of a barrier layer between the metal surface and the corrosive media [11].

3.2.2 Electrochemical analysis

3.2.2.1 Potentiodynamic polarization measurement

Evolution of the current density/potential in electrochemical experiments translates the inhibition efficiencies of the inhibitors in studied medium. Fig. 3 shows the Potentiodynamic polarization curves for the steel in 1 M hydrochloric acid solutions containing different concentrations of CC extract at 293 K after 30 min of immersion time. Table 2 presents the electrochemical kinetic parameters such as corrosion current density I (mA/cm²), corrosion potential Ecorr, cathodic and anodic Tafel slopes (b_c and b_a) and inhibition efficiency E%. Those parameters were determined by extrapolation method of the experiments curves.

The inhibition efficiency (E %) was calculated by:

$$E\,(\%) = \frac{I_{corr} - I'_{corr}(inh)}{I_{corr}} * 100 \qquad (3)$$

Where I_{corr} and I'_{corr} are corrosion density without and with presence of CC extract respectively.

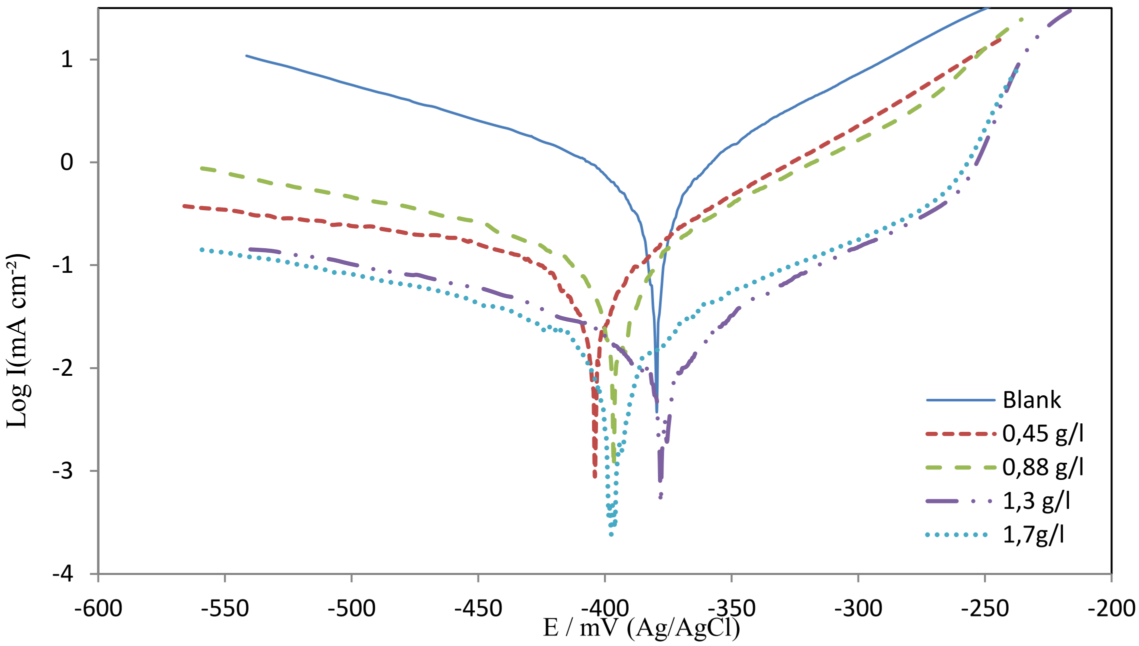

Fig. 3. Potentiodynamic polarization plots of steel immersed in 1M HCl with and without CC extract.

Examination of the polarization curves and electrochemical parameters show that the current density decreases significantly with the addition of the inhibitor in the acidic medium, yielding the increasing of inhibition efficiency (fig 4). In general, an inhibitor is an anodic or a cathodic if the variation E_{corr} against the blank is higher or above than 85 mV [6-20]. Since the largest displacement of the corrosion potential was about 26 mV (table 2), these results suggest that the studied inhibitors should be considered as a mixed-type inhibitor. Fig. 3 shows the parallel cathodic Tafel plots indicating that the hydrogen evolution is activation-controlled and the reduction mechanism is not affected by the presence of the inhibitor [21].

The cathodic hydrogen mechanism may be given below [22]:

$$Fe + H^+ \leftrightarrows (FeH^+)_{ads} \quad (4)$$

$$(FeH^+)_{ads} + e^- \rightarrow (FeH)_{ads} \quad (5)$$

$$(FeH)_{ads} + H^+ + e^- \rightarrow Fe + H_2 \quad (6)$$

The anodic plots are affected by the presence of the CC extract with concentration of 1.3 g/l. This means that the inhibitor can inhibit more efficiently the anodic dissolution of steel.

The following mechanism shows the corrosion of steel in acid solution [23-24]:

$$Fe + (OH^-)_{ads} \leftrightarrows Fe(OH^-)_{ads} + H^+(aq) \quad (7)$$

$$Fe(OH^-)_{ads} \rightarrow FeOH^+ + e^- \quad (8)$$

$$FeOH^+ + H^+ \leftrightarrows Fe^{2+} + H_2O \quad (9)$$

$(OH^-)_{ads}$ ions can be formed from the adsorbed water by:

$$(H_2O)_{ads} \rightarrow (OH^-)_{ads} + H^+(aq) \quad (10)$$

However, the corrosion process of steel in presence of inhibitor becomes:

$$Fe + Inh \leftrightarrows Fe(Inh)_{ads} \leftrightarrows Fe^{n+} + Inh + ne^- \quad (11)$$

Table. 1: Kinetic parameters derived from Potentiodynamic polarization plots of steel immersed in 1M HCl containing CC extract at 293K.

Conc.(g/l)	E_{corr} /mV(Ag/AgCl)	I_{corr}(mA/cm^2)	b_a(mV/dec)	b_c(mV/dec)	τ (%)
Blank	-379	0.6828	77.50	-142.90	---
0.45	-403	0.0875	72.90	-306.10	87.18
0.88	-400.7	0.0904	79.70	-196.00	87.00
1.30	-377.6	0.0171	82.70	-193.20	97.49
1.70	-396	0.0183	96.50	-201.10	97.31

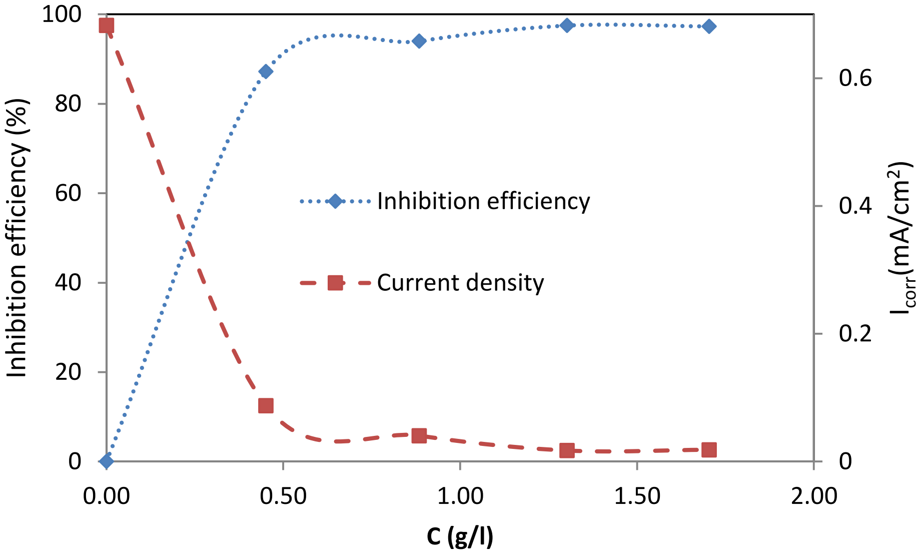

Fig. 4: Variation of the inhibitive efficiency and corrosion density against the CC extract at 293k.

In order to understand the electrochemical interfacial phenomena between the metal and the medium, we have analyzed the impedance diagrams.

3.2.2.2 Electrochemical impedance spectroscopy (EIS)

This technique is based on the perturbation of the electrochemical system around its operating point (E_{corr}, I_{corr}). The response of the system (ΔI) is sinusoidal and the electrochemical system acts as a linear electrical circuit [25]. EIS technique was studied to investigate the growth of the film formed on the steel surface by CC extract in 1 M HCl.

Fig. 5 shows the Nyquist plots for steel in 1HCl solution without and with different concentrations of the inhibitor at 293k after 30 min of immersion.

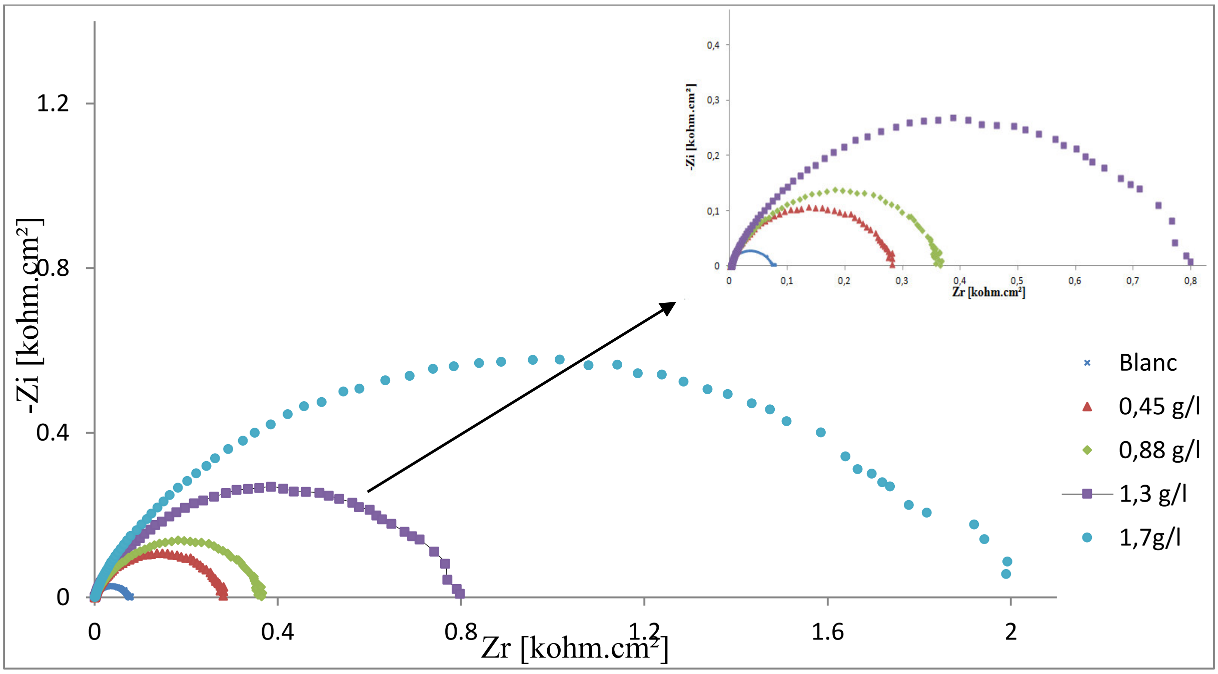

Fig. 5: Nyquist plots of steel immersed in 1M HCl with and without CC extract at 293K.

The analyses of the Nyquist plots conclude that the curves show a single capacitive semicircle exhibiting that the corrosion process was mainly charge-transfer controlled [26]. The curves shape doesn't change with the inhibitor concentration, indicating that the corrosion mechanism doesn't under go any change [9]. In all cases capacitive loops whose diameter increased significantly with the addition of the concentrated inhibitor (fig 5). In other words, the charge transfer resistance increases with the CC extracts concentration.

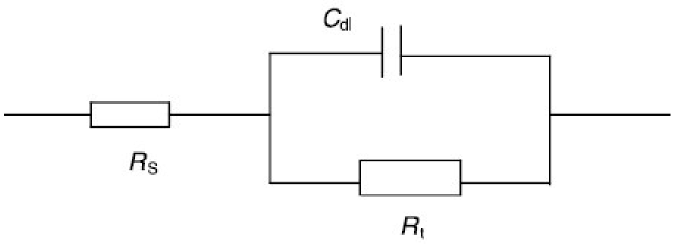

Fig. 6. Equivalent electrical circuit of the interface of steel /HCl electrolyte.

The impedance parameter values of charge transfer resistance (R_{ct}), double layer capacitance (C_{dl}) and inhibition efficiency are listed in table 2. The Nyquist plots were analyzed by fitting experimental data in the equivalent electrical circuit shown in fig 6.

The inhibition efficiency (E %) was calculated by:

$$\text{E (\%)} = \frac{R'_{ct}(inh) - R_{ct}}{R_{ct}(inh)} * 100 \tag{12}$$

Table. 2: Kinetic parameters derived from Nyquist plots of steel immersed in 1 M HCl at different concentrations of CC extract at 293k.

Conc.(g/l)	R_{ct}(Ω.Cm^2)	C_{dc}(μF/Cm^2)	τ (%)
Blank	58.30	172.5	---
0.45	228.8	34.82	79.75
0.88	374.5	16.99	89.69
1.30	791.9	11.25	92.60
1.70	2005	5.651	97.09

The examination of the results indicates that the introduction of the CC extract increases the R_{ct} from 58.3 to 2005 Ω.Cm^2, at the same time; it decreases the C_{dl} from 172.5 to 5.65µF/Cm^2. This evolution of charge transfer resistance indicates the high adsorption of inhibitor and formation of the surface film on the steel in order to prevent the dissolution of the metal [27]. For the double layer capacitance, the values decrease with the increasing of the concentration inhibitor. This Cdl decreasing can be related to a reduction in local dielectric and/or thickness increasing of electrical double layer. Hence, we can conclude that these results suggest the increasing of inhibition efficiency [27-28].

The Potentiodynamic polarization and Nyquist measurements analyze show a satisfactory agreement.

3.3 Thermodynamic parameters

It is clear that the corrosion current density of steel in 1M HCl solution increases with the temperature increase. Table 3 exhibits that the inhibition efficiency decreases with the temperature increase. In order to examine the corrosion process and the thermodynamics of adsorption of our inhibitor, we have investigated the variation of the temperature with the corrosion current density, using Tafel extrapolation method.

The corrosion reaction can be studied as an Arrhenius-type process using the following relation:

$$I_{corr} = A.e^{\frac{-E_a}{R.T}} \tag{13}$$

Where I_{corr} is the corrosion current density of steel, Ea is the apparent activation energy, A is constant, R is the universal gas constant and T is the absolute temperature.

$$I_{corr} = \frac{TR}{hN} exp\left(\frac{\Delta S^*_a}{R}\right) exp\left(-\frac{\Delta H^*_a}{RT}\right) \tag{14}$$

Where h is Planck's constant, N is Avogadro's number, ΔS^*_a is the entropy of activation, ΔH^*_a is the enthalpy of activation, T is the absolute temperature and R is the universal gas constant.

Table. 3. The influence of temperature on the electrochemical parameters for steel electrode immersed in 1 M HCl and 1 M HCl + 1.3 g L-1 of CC extract.

	T(K)	I(mA/Cm^2)	E_{corr}/mV (Ag/AgCl)	Ba (mV)	Bc (mV)	E(%)
Blank	20	0.6828	-379	77.5	-142.9	--
	30	0.8968	-376.9	84.2	-181.2	--
	40	1.2469	-388	87.2	-201.2	--
	50	2.6771	-401.9	133.3	-121.6	--
Plant extract	20	0.0171	-377.6	82.7	-193.2	97.49
	30	0.0229	-400.1	84.5	-113.9	97.44
	40	0.0918	-419.6	104.2	-224.2	92.62
	50	0.8791	-433.7	134	-145.3	67.16

Fig. 7 shows the evolution of Ln (Icorr) against 1/T with and without inhibitor will give a straight line of slope $-E_a/R$, which enables to calculate the apparent activation energy with and without the inhibitor. Table 4 shows that the lower values of apparent activation energy in 1M HCl solution beside the presence of the inhibitor. The increased in apparent activation energy in presence of inhibitor compared to free acid solution (34.51 to 102.67 KJ/mol) indicates the low performance of the inhibitor at higher temperature. This evolution can be interpreted by an electrostatic adsorption process of the inhibitor on the steel surface (physical adsorption) [21-29].

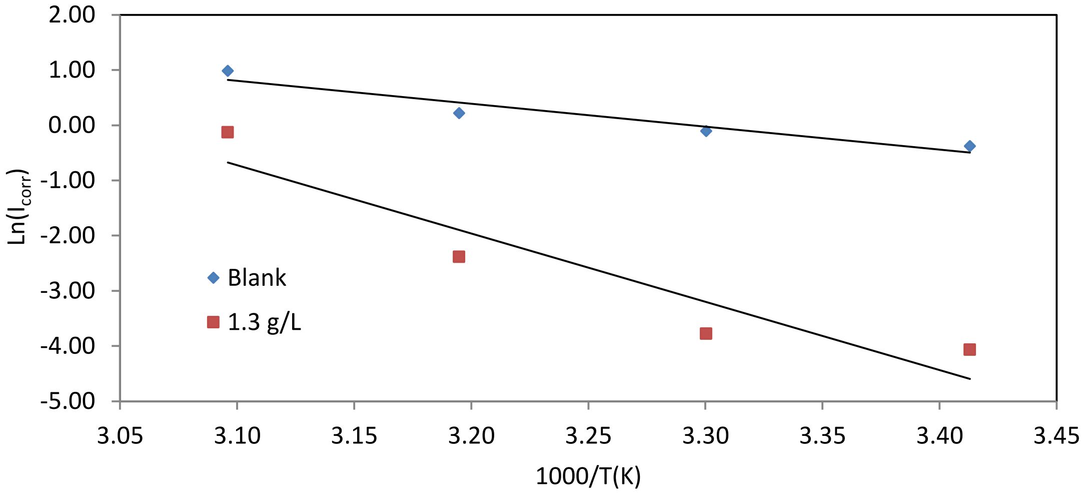

Fig. 7. Arrhenius plots of Ln (I_{corr}) vs. 1/T (K^{-1}) in 1 M HCl with and without 1.3g/l of CC extract

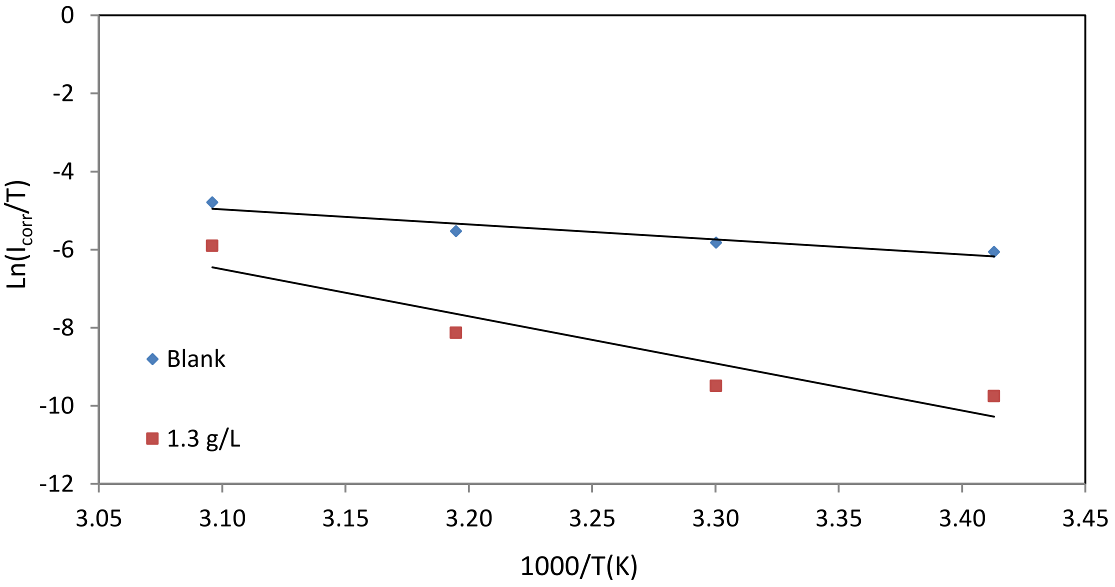

Fig. 8. Transition-state plots of Ln(I_{corr}/T) vs. 1/T (K^{-1}) in 1M HCl with and without 1.3 g/l of CC extract.

Fig 8 indicates the variation of Ln (I_{corr}/T) versus 1/T. The slope equal to $-\Delta H^{*}_{a}/R$ and the intercept to $Ln\frac{R}{hN}+\frac{\Delta S}{R}$ from which we can calculate ΔS^{*}_{a} and ΔH^{*}_{a} values that given in table 4.

The positive sign of ΔH^{o}_{ads} shows the endothermic nature of the S300 steel dissolution process. However the value of ΔH^{o}_{ads} in presence of inhibitor is more important than those obtained without the inhibitor. It have been reported that this evolution attributes this evolution of the enthalpy of physical adsorption of inhibitor on the metal surface [30]. The values of the entropy given in table 4 explain that ΔS^{o}_{ads} increases more positively in the presence of the inhibitor compared to free acid solution. This value of entropy of activation highlights an increase in disordering take place in presence of the inhibitor [31].

We remark the same evolution between ΔH^{o}_{ads} and E_a values (Table 4). This result explains the thermodynamic relation between these parameters by the follow relation:

$$E_a - \Delta H^{\circ}_{a} = RT \quad (15)$$

Table. 4. Activation data of corrosion reaction of steel in 1M HCl with and without the CC extract.

Inhibitor	E_a (KJ/mol)	ΔH^o_{ads} (KJ/mol)	ΔS^o_{ads} (J/mol.K)	E_a -ΔH^o_{ads}
1M HCl	34.51	32.01	-139.601	2.5
CC extract	102.67	100.304	59.363	2.4

3.4 Adsorption isotherms

The application of adsorption isotherms allow to analyze the interaction mode in the inhibition process between adsorbent and adsorbed [32]. In order to start this adsorption, the surface coverage (θ) was evaluated by using the inhibition efficiency values from polarization studies. The surface coverage increased with the increasing of CC extract concentration, therefore the adsorbed molecules on the metal surface. The surface coverage (θ) with different concentrations of CC extract was tested by different adsorption isotherms such as Langmuir, Temkin and Freundlich. The Langmuir isotherm is the best model that fitted our inhibitor with correlation coefficients (R2) equal to 0.9944 (Table 5).

The Langmuir isotherm assumed that the adsorbed molecules occupy only one site and there was no interaction with other adsorbed molecules in metal surface [33].

The surface coverage (θ) is calculated using the following relation:

$$\theta = \frac{I_{corr} - I_{corr}^{inh}}{I_{corr}} \tag{16}$$

The Langmuir isotherm is given by the following relation:

$$\frac{\theta}{1-\theta} = K_{ads}C_{inh} \tag{17}$$

$$\frac{C_{inh}}{\theta} = \frac{1}{K_{ads}} + C_{inh} \tag{18}$$

Temkin isotherm :

$$\theta = \frac{RT}{b_T} ln(K_T.C) \tag{19}$$

Freundlich isotherm

$$log\theta = logK_F + n_F logC \tag{20}$$

Where θ is the surface coverage, C_{inh} is the concentration of the inhibitor and K_{ads} is the standard adsorption equilibrium constant that related to the standard free energy of adsorption ΔG°_{ads} by the following relation:

$$\Delta G^{\circ}_{ads} = -2{,}303RTlog(55{,}5.K_{ads}) \tag{21}$$

Where 55.5 is the molar concentration of water in the solution, R is the gas equilibrium constant and temperature T is 293K.

Fig. 9 shows the linear evolution plots of C/θ against C where the slope is 0.963. This result suggests that the inhibitor occupied about 0.963 adsorption sites on the metal surface [32-34]. The linear correlation coefficients near to 1 (R^2=0.994) means that the adsorption of inhibitor on S300 steel fulfills the Langmuir isotherm and each site holds one adsorbed species.

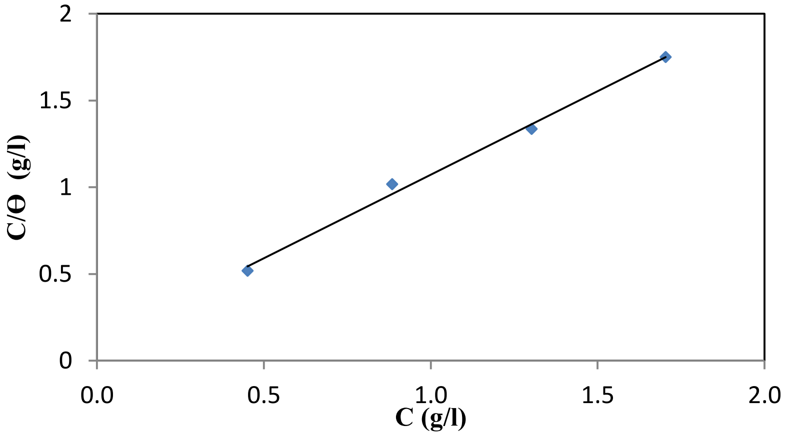

Fig 9. Langmuir adsorption plots for steel in 1 M HCl solution containing different concentrations of CC extracts at 293k.

Table. 5. Parameters of adsorption models and coefficients of determination at 293K.

Isotherm	R^2	Slope	Intercept	K_{ads}		ΔG°_{ads} (kJ/mol)
Langmuir	0.9944	0.9631	0.1099	9.0991	-	-15.17
Temkin	0.7223	0.0877	0.9251	38.118	b_T 27.77	-18.65
Freundlich	0.7219	0.0951	-0.0794	0.8329	n 10.51	-9.34

The negative values of ΔG°_{ads} given in Table 5 explains spontaneous adsorption of the inhibitor on the steel surface and the stability of the adsorbed layer on the steel surface [22-35].

Generally, ΔG°_{ads} with values around -20kJ mol-1 or low correspond to electrostatic interaction between charged molecules of inhibitor and metal surface (physical adsorption); ΔG°_{ads} of -40KJ mol-1 or low means that the inhibitor molecules involve charge sharing or transferring to the metal surface to form a coordinate covalent bond (chemical adsorption) [36]. The table 5 shows the standard free energy of adsorption ΔG°_{ads}values that can be calculated as -15.17 kJ mol-1 from Eq.(9). The lower value of ΔG°_{ads} suggested that the interaction between inhibitor molecules and metal surface as a physical adsorption by formation of an adsorptive film with electrostatic character [37].

4. Conclusions

- In this work, we conclude from the results that the *CC* extracts exhibit good inhibition properties for S300 steel in 1 M HCl. The inhibition efficiency values increase with the inhibitor concentration with a maximum 97.7% at 1.3 g L^{-1},
- Inhibitor acts as a mixed mode of inhibition as is indicated by Tafel polarization studies,
- The apparent activation energy and enthalpy of activation increase in the presence of the inhibitor compared to free acid solution. Enthalpy of activation highlights the endothermic nature of the steel dissolution process, accompanied by an increase of entropy.
- The adsorption of *Cuminum cyminum* extract fulfills Langmuir adsorption isotherm,
- The data obtained from Tafel polarization, electrochemical impedance spectroscopy and gravimetric methods are in good agreement.

References

1. Koch, Gerhardus H., et al. (2002). "Cost of corrosion study unveiled." *Supplement to Materials Performance* 2.
2. LANDOLT, Dieter. (1997) "Corrosion et chimie de surfaces des métaux". PPUR presses polytechniques.
3. Hmamou, Dris Ben, et al. "Carob seed oil: an efficient inhibitor of C38 steel corrosion in hydrochloric acid." *International Journal of Industrial Chemistry* 3.1 (2012): 1-9.
4. Ibisi, N. E., V. I. Ngwamaghi, and D. O. Okoroafor. "Eco-Friendly Corrosion Inhibitors: Adsorption And Inhibitive Action Of Ethanol Extracts Of Mallotus Oppositifolius Leaves For The Corrosion Of Mild Steel In 1m Hydrochloric Acid Solution." (2015).
5. Helen, L. Y. S., et al. "Aquilaria Crassna Leaves Extracts–a Green Corrosion Inhibitor for Mild Steel in 1 M HCl Medium." Int. J. Electrochem. Sci 9 (2014): 830-846.
6. Bammou, L., et al. "Corrosion inhibition of steel in sulfuric acidic solution by the chenopodium ambrosioides extracts." Journal of the Association of Arab Universities for Basic and Applied Sciences 16 (2014): 83-90.
7. Yousfi, F., et al. "Zingiber Officinal Roscoe Extract Using as Green Corrosion inhibitor for Mild Steel in 1M HCl Media." (2015).
8. Victoria, S. Noyel, Rohith Prasad, and R. Manivannan. "Psidium Guajava Leaf Extract as Green Corrosion Inhibitor for Mild steel in Phosphoric Acid." Int. J. Electrochem. Sci 10 (2015): 2220-2238.
9. I. Hamdani et al. "Chemical constituents and corrosion inhibition of mild steel by the essential oil of Thymus algeriensis in 1.0 M hydrochloric acid solution." Der Pharma Chemica, (2015), 7 (8):252-264
10. Saxena, Archana, et al. "Corrosion Inhibition and Adsorption Behavior of Clove Oil on Iron in Acidic Medium." Journal of Chemistry 9.4 (2012): 2044-2051.
11. Obot, I. B., N. O. Obi-Egbedi, and N. W. Odozi. "Acenaphtho [1, 2-b] quinoxaline as a novel corrosion inhibitor for mild steel in 0.5 MH 2 SO 4."Corrosion Science 52.3 (2010): 923-926.
12. M. A. Quraishi, F. A. Ansari, D. Jamal. "Thiourea derivatives as corrosion inhibitors for mild steel in formic acid." Materials Chemistry and Physics, 77 (2003) 687–690.
13. Li, W., Zhao, X., Liu, F., & Hou, B. (2008). "Investigation on inhibition behavior of S-triazole–triazole derivatives in acidic solution." Corrosion Science, 50(11), 3261-3266.
14. Rong Li and Zi-Tao Jian, Chemical composition of the essential oil of Cuminum cyminum L. from China Flavour Fragr. J. 2004; 19: 311–313.

15. Hui Cang et al., " Inhibition Effect of Reed Leaves Extract on Steel in Hydrochloric Acid and Sulphuric Acid Solutions" Int. J. Electrochem. Sci., 7 (2012) 8869 – 8882.
16. Gunasekaran, G., and L. R. Chauhan. "Eco friendly inhibitor for corrosion inhibition of mild steel in phosphoric acid medium." Electrochimica Acta 49.25 (2004): 4387-4395.
17. Li, X., Deng, S., & Fu, H. (2012). Inhibition of the corrosion of steel in HCl, H 2 SO 4 solutions by bamboo leaf extract. Corrosion Science, 62, 163-175.
18. Obiukwu, O. O., I. O. Opara, and B. C. Oyinna. " Corrosion Inhibition of Stainless Steel Using Plant Extract Vernoniaamygdalina and Azadirachtaindica." Pacific Journal of Science and Technology 14 (2013): 31-35.
19. Osita O, et al,"Corrosion Inhibition of Mild Steel by Various Plant Extracts in Acid Media", Res. J. Appl. Sci. Eng. Technol., 10(10): 1197-1205, (2015).
20. Zhang, J., Gong, X.L., Yu, H.H., Du, M. The inhibition mechanism of imidazoline phosphate inhibitor for Q235 steel in hydrochloric acid medium. Corros. Sci. 2011 53, 3324–3330.
21. Afia, Leila, et al. "Argan hulls extract: green inhibitor of mild steel corrosion in 1 M HCl solution." Research on Chemical Intermediates 38.8 (2012): 1707-1717.
22. DÖNER, Ali, SOLMAZ, Ramazan, ÖZCAN, Muzaffer, et al. Experimental and theoretical studies of thiazoles as corrosion inhibitors for mild steel in sulphuric acid solution. Corrosion Science, 2011, vol. 53, no 9, p. 2902-2913.
23. Natalya V. Likhanova, Corrosion Inhibition of Carbon Steel in Acidic Environment by Imidazolium Ionic Liquids Containing Vinyl-Hexafluorophosphate as Anion. Int. J. Electrochem. Sci., 6 (2011) 4514 – 4536
24. R. Fuchs-Godec, Colloids Surf. A Physicochem. Eng. Aspects, 280 (2006) 130.
25. Wang, H. B., Shi, H., Hong, T., Kang, C., & Jepson, W. P. (2001). CORROSION 2001.
26. R. Rosliza, W.B. Wan Nik, H.B. Senin, Mater. Chem. Phys. (2008), 107, 281.
27. L. Afia. al . Application of Argan plant extract as green corrosion inhibitor for steel in 1 mol/L HCl. Acta Metall. Sin.(Engl. Lett.)Vol.25 No.1 pp10-18 February (2012).
28. Ashassi-Sorkhabi, H., B. Shaabani, and D. Seifzadeh. "Effect of some pyrimidinic Shciff bases on the corrosion of mild steel in hydrochloric acid solution." Electrochimica Acta 50.16 (2005): 3446-3452.
29. MARTINEZ, Sanja et STERN, Ivica. Thermodynamic characterization of metal dissolution and inhibitor adsorption processes in the low carbon steel/mimosa tannin/sulfuric acid system. Applied Surface Science, (2002), vol. 199, no 1, p. 83-89.
30. A. Zarrouk. Temperature Effect, Activation Energies and Thermodynamic Adsorption Studies of L-Cysteine Methyl Ester Hydrochloride As Copper Corrosion Inhibitor In Nitric Acid 2M. Int. J. Electrochem. Sci., 6 (2011) 6261 – 6274
31. Sudhish K. Shukla, Eno E. Ebenso. Corrosion Inhibition, Adsorption Behavior and Thermodynamic Properties of Streptomycin on Mild Steel in Hydrochloric Acid Medium. Int. J. Electrochem. Sci., 6 (2011) 3277 – 3291
32. W.A.W. Elyn Amira, Corrosion Inhibition of Mild Steel in 1 M HCl Solution by Xylopia Ferruginea Leaves from Different Extract and Partitions, Int. J. Electrochem. Sci., 6 (2011) 2998 – 3016.
33. M.G. Hosseini, S.F.L. Mertens and M.R. Arshadi, Corros. Sci., 45 (2003) 1473.
34. L. Larabi, Y. Harek, O. Benali and S. Ghalem, Progress in Organic Coatings, 54 (2005) 256.
35. M.J. Bahrami, S.M.A. Hosseini, P. Pilvar, Experimental and theoretical investigation of organic compounds as inhibitors for mild steel corrosion in sulfuric acid medium, Corros. Sci. 52 (2010) 2793–2803.
36. N.A. Negm, Y.M. Elkholy, M.K. Zahran, S.M. Tawfik, Corrosion inhibition efficiency and surface activity of benzothiazol-3-ium cationic Schiff base derivatives in hydrochloric acid, Corros. Sci. 52 (2010) 3523–3536.
37. R.solmaz et al. Acta physic-Chimica sinica, (2008), 24(7): 1185-1191.